Int. J. Heat Mass Transfer. Vol. 20, pp. 1051–1058. Pergamon Press 1977. Printed in Great Britain

APPLICATION OF THE HOT WIRE ANEMOMETER TO TEMPERATURE MEASUREMENT IN TRANSIENT GAS FLOWS

T. I. EKLUND* and R. A. DOBBINS†

(*Received* 14 *July* 1976 *and in revised form* 20 *December* 1976)

Abstract—The application of the hot wire anemometer to the measurement of temperature in transient gas flows is developed and demonstrated. Corrections for temperature dependent gas properties and heat loss to the hot wire supports are discussed and incorporated in the analysis. Design criteria are developed to minimize errors and allow static calibration of the wires. Operational characteristics of the anemometer are considered, and an error analysis demonstrates main areas of improvement. Sample data traces and reduced data for expansions of dry argon and water saturated argon in a Wilson cloud chamber are provided.

NOMENCLATURE

A_c, hot wire sensor cross section;
$\mathscr{A}_i$, amplification of the bridge amplifier (see discussion, Appendix A);
D, hot wire sensor diameter;
h_i, convective heat-transfer coefficient;
I, electric current through sensor;
I_A, I_B, I_P, influence coefficients defined in text;
k, gas thermal conductivity;
k_w, thermal conductivity of sensor material;
l, length of sensor;
l_c, cold length defined in text;
Nu_f, Nusselt number based on film temperature equal hD/k_f;
p, pressure;
P, electrical power supplied to sensor equal to heat transferred to ambient gas;
$\mathscr{P}_r$, reduced power ratio defined in text;
R, resistance of sensor at temperature T;
R_g, gas constant;
R_0, resistance of the sensor at temperature T_0;
S, sensor surface area;
T_f, film or average temperature $(T+T_\infty)/2$;
T_i, temperature of sensor wire where i refers to sensor A or B;
T_0, a reference temperature here taken to be the initial temperature;
T_∞, ambient gas temperature;
U, gas velocity;
V, anemometer output voltage;
V_{ref}, the amplified bridge unbalance voltage which is termed the reference voltage;

Greek symbols

α_i, temperature coefficient of resistance of sensor i;
γ, ratio of specific heats;
ΔR_i^{ap}, the apparent sensor resistance increment which is set by the control resistance decade designated as R_1 in Fig. 1;
ΔR_i^{cor}, the correction to the sensor resistance owing to the unbalance of the bridge;
$\Delta T_A^{(i)}$, $= T_A^{(i)} - T_0$, where i refers to the iteration;
$\Delta T_B^{(i)}$, $= T_B^{(i)} - T_0$, where i refers to the iteration;
$\Delta T_\infty^{(i)}$, $= T_0 - T_\infty^{(i)}$ where i refers to the iteration;
ε, relative error of a given parameter;
θ, temperature difference between sensor and gas, $T - T_\infty$;
μ_f, dynamic viscosity at the film temperature;
ρ, gas density at the film temperature;
σ, specific resistance of sensor material.

Subscripts

fi, refers to the film temperature defined in the test of sensor i;
i, refers to sensor A or B;
is, refers to values obtained by the isentropic relationship;
0, refers to the initial temperature.

1. INTRODUCTION

IN A PREVIOUS study [1], the method of Laplace was used to facilitate the experimental determination of homogeneous nucleation rates. That analysis indicated the desirability of obtaining time-resolved measurements of temperature in the supersaturated, expanding gas of a Wilson cloud chamber. While the isentropic law has been employed in the past to obtain temperature from instantaneous pressure measurements [2, 3], its use during the nucleation event is questionable. Thus, the need remains for a temperature sensing technique which is applicable when departures from isentropic flows are prominent. In particular, during nucleation when transport phenomena guarantee non-isentropic behavior the need for a precise measurement of temperature is of paramount importance. This study develops a technique for applying hot wire anemometry

*Aerospace Engineer, Department of Transportation, Federal Aviation Administration, National Aviation Facilities Experimental Center, Atlantic City, NJ 08405, U.S.A.

†Professor of Engineering, Brown University, Providence, RI 02912, U.S.A.

to temperature measurement in the supersaturated, expanding gas of the Wilson cloud chamber. The results may be applicable to a variety of other experiments.

When temperature measurements are made in transient phenomena, the measuring element is normally a thermocouple or resistance wire constructed small enough so that it lags the true environmental temperature by some acceptably small increment. This type measurement is useless in supersaturated gases, as condensation may occur on the sensor and the associated latent heat release causes the sensor to indicate an incorrect temperature.

Of potential application to this problem is the conventional hot wire anemometer, whereby the sensor is maintained at some constant temperature above the test gas dew point. Since the sensor does not follow the actual environmental temperature, the total heat transfer from the wire is the measured parameter. If a single hot wire sensor is used, an accurate temperature resolution would demand a precise knowledge of heat-transfer laws, the properties of the ambient fluid, and wire properties. In steady state flows such as exist in wind tunnels, these extensive requirements are circumvented by calibration of the wire at known conditions. In transient expansions, the conventional calibration techniques are inapplicable. The transient experiment in principle becomes more tractable if two hot wire sensors are operated at different temperatures. The heat transfer of each is related to the temperature difference between the respective wire and the ambient gas temperature which is then determined.

2. THE HOT WIRE TECHNIQUE

Figure 1 presents a schematic diagram of a typical anemometer unit that is designed to function in the constant temperature mode. The role of the amplifier is to maintain a nearly zero voltage difference between points A and C on the bridge despite variations of the cooling rates of the sensing wire that is located between terminals A and D. If the wire resistance is set at the

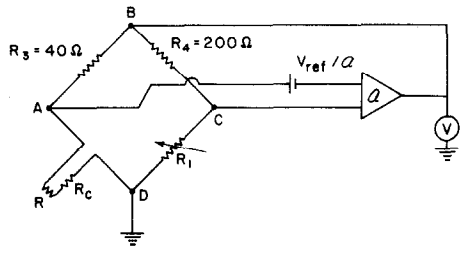

FIG. 1. Constant temperature anemometer bridge with amplifier.

value R corresponding to the temperature T, any drop in sensor temperature results in a voltage unbalance between A and C. The amplifier then increases the bridge output voltage V that is measured between B and D, thereby passing more current through both legs of the bridge and heating the sensor to its former resistance value.

Elementary circuit theory gives the power P supplied to the heated wire as

$$P = \frac{RV^2}{(R+R_c+R_3)^2} \tag{1}$$

where R is the pre-set sensor resistance, R_c is the cable plus sensor support resistance, and R_3 is the resistance between terminals A and B of the bridge. This electrical power provides the heat transfer from the hot wire to the gas which may be expressed as

$$P = hS(T-T_\infty). \tag{2}$$

If two sensors are used and their temperatures are designated as T_A and T_B then we may write

$$P_i = h_i S_i (T_i - T_\infty) \tag{3}$$

where $i = A, B$. Accordingly we find the dimensionless temperature ratio is

$$\frac{T_B - T_\infty}{T_A - T_\infty} = \mathscr{P}_r \tag{4}$$

with

$$\mathscr{P}_r = \frac{P_B}{P_A}\frac{h_A}{h_B}\frac{S_A}{S_B}$$

and

$$P_i = \frac{R_i V_i^2}{(R_i + R_{ci} + R_{3i})^2}, \quad i = A, B.$$

In practice the sensor temperatures are measured with respect to the well established initial temperature T_0. We define the temperature differences $\Delta T_A \equiv T_A - T_0$, $\Delta T_B \equiv T_B - T_0$, $\Delta T_\infty \equiv T_0 - T_\infty$ and equation (4) is then expressed as

$$\frac{\Delta T_\infty + \Delta T_B}{\Delta T_\infty + \Delta T_A} = \mathscr{P}_r \tag{5}$$

or

$$\Delta T_\infty = \frac{1}{\mathscr{P}_r - 1}\Delta T_B - \frac{\mathscr{P}_r}{\mathscr{P}_r - 1}\Delta T_A. \tag{6}$$

Thus, if the ratio $h_A S_A / h_B S_B$ is known, the measurement of the output voltages V_i and the knowledge of the various resistances yields $\mathscr{P}_r$ and, with ΔT_B and ΔT_A known, the value of ΔT_∞ is found from equation (6). An iterative procedure is used, as described below, to determine ΔT_∞ in order to incorporate several corrections which depend on the magnitudes of the initially unknown convective heat-transfer coefficients h_i and the unknown temperature T_∞.

The area ratio S_B/S_A is determined by a test in which both wires are run at precisely the same temperature. In this case since $h_A = h_B$ and $T_A = T_B$ we find from equation (4) that

$$\frac{S_A}{S_B} = \frac{P_A}{P_B}.$$

In setting $T_A = T_B$ it is usually necessary to include the small correction for the bridge imbalance that is discussed below. This equal overheat test was performed during a cloud chamber expansion as a check on the performance of the system under dynamic conditions.

The sensors will be maintained by the anemometer bridge circuit at nearly constant resistances which are related to their respective temperatures by

$$R_i = R_{0i}[1+\alpha_i(T_i - T_0)] \tag{7}$$

where $i = A$ and B. The feedback circuit operates by sensing a finite bridge imbalance. The result of the presence of the imbalance is that the sensor resistances and temperatures are actually higher than the values indicated by the anemometer units. Circuit theory (see Appendix A) leads to the resistance correction

$$\Delta R_i^{corr} = \left(\frac{V_{ref}}{V} - 1\right)\frac{(R_{0i}+\Delta R_i^{ap}+R_{ci}+R_3)^2}{\mathscr{A}_i R_3}. \tag{8}$$

The true sensor resistance may be calculated by

$$R_i = R_{0i}+\Delta R_i^{ap}+\Delta R_i^{cor}. \tag{9}$$

The quantity ΔR_i^{ap} is the resistance increment that is added by increasing the variable R_1 above the zero overheat value. The first estimate of temperature is found by setting ΔR_i^{ap} for sensors A and B, then determining ΔR_i^{cor} and R_i from equations (8) and (9). For this first iteration we assume $h_A = h_B$ and that heat conduction along the sensors to the support wires can be ignored. Thus we write

$$\frac{\Delta T_\infty^{(1)}+\Delta T_B^{(1)}}{\Delta T_\infty^{(1)}+\Delta T^{(1)}} = \mathscr{P}_r^{(1)} \tag{10}$$

where

$$\mathscr{P}_r^{(1)} = \frac{P_B S_A}{P_A S_B}. \tag{11}$$

A. *The correction for* $h_B/h_A \neq 1$

Because the sensors temperatures are unequal the convective heat-transfer coefficients are not identical. The study of Collis and Williams [4] provides a basis for the determination of h_B/h_A through the use of their relationship for the heat transfer between fine wires and a surrounding gas,

$$\frac{hD}{k} = \left(\frac{T_f}{T_\infty}\right)^{0.17}\left[0.24+0.56\left(\frac{\rho UD}{\mu_f}\right)^{0.45}\right]. \tag{12}$$

Although this relationship was verified for experiments with air its applicability for other gases is herein presumed. The influence of gas composition on convective heat-transfer rate is through the properties indicated in equation (12) plus an additional factor equal to the Prandtl number raised to the 1/3 power. For most all gases this additional correction is not significant in the present context. For wires A and B the ratio of convective heat-transfer coefficients therefore is given by

$$\frac{h_B}{h_A} = \left(\frac{T_{fB}}{T_{fA}}\right)^{1.01}\frac{\left[0.24+0.56\left(\frac{\rho UD}{\mu(T_{fB})}\right)^{0.45}\right]}{\left[0.24+0.56\left(\frac{\rho UD}{\mu(T_{fA})}\right)^{0.45}\right]} \tag{13}$$

where

$$T_{fi} = \frac{T_i^{(1)}+T_\infty^{(1)}}{2}, \quad i = A, B \tag{14}$$

and we have used

$$k = k_{ref}\left(\frac{T_f}{T_{ref}}\right)^{0.84} \tag{15}$$

$$\mu = \mu_{ref}\left(\frac{T_f}{T_{ref}}\right)^{0.85} \tag{16}$$

and

$$\rho = P/R_g T_\infty^{(1)}. \tag{17}$$

Thus, we define the second iteration of the reduced power as

$$\mathscr{P}_r^{(2)} = \mathscr{P}_r^{(1)}\frac{h_A}{h_B} \tag{18}$$

and find the second iteration of dimensionless temperature given by

$$\frac{\Delta T_\infty^{(2)}+\Delta T_B^{(1)}}{\Delta T_\infty^{(2)}+\Delta T_A^{(1)}} = \mathscr{P}_r^{(2)} \tag{19}$$

and the corresponding revision to equation (6).

B. *The correction for heat conduction to the support wire*

The correction due to heat conduction from the hot wire to the support wire is based on a fin-type heat-transfer analysis. The conduction correction here differs somewhat from other treatments and their results [5, 6] because in the steady flows considered in most hot wire work, the support wire temperature is equal to the free stream gas temperature. The hot wire is treated as a fin projecting from a support of known temperature, T_0, into a gas of known temperature, T_∞, and a quasi-steady solution is employed (see Fig. 2). The

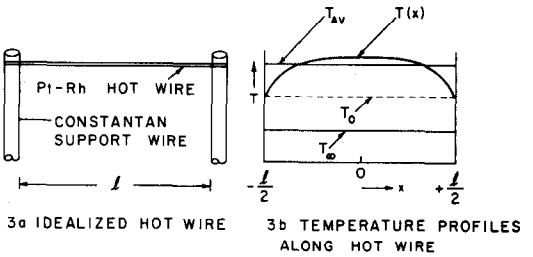

FIG. 2. Temperature profile of hot wire sensor.

classical equation for fin cooling with an internal heat source results

$$\frac{d^2\theta}{dx^2} - \frac{\pi Dh}{k_w A_c}\theta + \frac{I^2\sigma_w}{k_w A_c} = 0 \tag{20}$$

where $\theta = T - T_\infty$ is the local difference in temperature between the wire and the free stream. The boundary conditions are $d\theta/dx = 0$ at the center of the wire where $x = 0$, $\theta_0 = T_0 - T_\infty$ at $x = \pm l/2$ where l is the wire length and T_0 is the support temperature which equals the initial test gas temperature. In the analysis, σ_w, h and k_w are all taken as constants.

Since the resistance of the wire is held nearly constant by the anemometer unit, the average wire temperature and hence $(\theta_{ave}+T_\infty)$ is a pre-set constant provided the wire resistance is a linear function of temperature.

The solution to equation (20) with the prescribed boundary conditions for the average wire temperature is

$$\theta_{ave} = \left(\theta_0 - \frac{P}{hS}\right)\frac{l_c}{l}\tanh\frac{l}{l_c} + \frac{P}{hS} \tag{21}$$

where the cold length is defined by

$$l_c \equiv 2\left(\frac{K_w A_c}{Dh}\right)^{1/2} = \frac{D}{Nu_f^{1/2}}\left(\frac{K_w}{K_f}\right)^{1/2}. \tag{22}$$

For the long sensors used in this study the ratio $l/l_c \gg 1$ and $\tanh(l/l_c) \approx 1$. Therefore, for each wire we write

$$T_\infty = T_{i,ave}\left(1+\frac{l_c}{l}\right)_i - T_0\left(\frac{l_c}{l}\right)_i - \left(\frac{P}{hs}\right)_i \tag{23}$$

where $i = A, B$.

Accordingly,

$$\frac{T_{B,ave}\left(1+\frac{l_c}{l}\right)_B - T_\infty - T_0\left(\frac{l_c}{l}\right)_B}{T_{A,ave}\left(1+\frac{l_c}{l}\right)_A - T_\infty - T_0\left(\frac{l_c}{l}\right)_A} = \frac{P_B h_A S_A}{P_A h_B S_B}. \tag{24}$$

This expression can be recast as

$$\frac{\Delta T_\infty^{(3)} + \Delta T_B^{(2)}}{\Delta T_\infty^{(3)} + \Delta T_A^{(2)}} = \mathscr{P}_r^{(2)} \tag{25}$$

where

$$\Delta T_i^{(2)} = (\Delta T_i^{(1)})(1 + l_c/l)_i. \tag{26}$$

The quantity $\Delta T_i^{(2)}$ given by equation (26) is equal to the average sensor temperature minus the initial temperature T_0. Thus equation (25) will reduce to equation (19) for the second iteration $\Delta T_\infty^{(2)}$ when the cold length correction is negligible. For our results the correction for conduction effects is usually small because the sensor wires are relatively long. It should be noted that the cold length correction vanishes when both wires are run at identical temperatures to establish S_B/S_A if their lengths are the same.

The lengths of the sensor wires were calculated from the measured resistances and the specific resistance σ_w at the measured temperature. The physical constants of the wire that were used in calculating l_c/l were $k_w = 30\,\mathrm{W/m^2\,K}$ and $\sigma_w = 21.1 \times 10^{-8}\,\Omega\,\mathrm{m}$ at 273.2 K [7].

3. PROBE CONSTRUCTION AND USE

The dual sensor probe assembly is designed in such a way that both sensors lie in a plane that is perpendicular to the oncoming flow with their centers 10 mm apart. Each sensor wire was made of platinum (90%)–rhodium (10%) Wollaston wire of 5 μm dia. The sensors were at least 6 mm in length to reduce the error due to heat conduction to the supports. The influence of the thermal boundary layer of the supports was minimized by mounting the sensors on the upstream side of the support. The sensors were mounted with as little bowing as possible and the flow velocity was small enough so that the strain-gauge effect from aerodynamic drag on the wire should be negligible [6]. For the tests described below, the hot wires were positioned midway between the center of the chamber and the walls. In this manner, the wires were kept free of the thermal boundary layer at the wall and the wake shed by the centerline electrode. Temperature of the wire is accurately set by adjusting a variable decade control resistance R_1 on the opposite leg of the anemometer bridge.

The probe support wires were made of 0.40 mm dia constantan wire and were electrically isolated from each other. Constantan was used because of its low temperature coefficient of resistance. This was important as the entire probe was placed in a capsule and immersed in well-stirred bath of precisely controlled temperature for determination of α_i for each sensor. During calibration the probe support wires have a temperature equal to the hot wire, while during the actual test the support wires maintain the initial test gas temperature because of their large thermal inertia. Constantan has a negligible change in resistance over the temperature range involved and this prevents an error in the measurement of α_i owing to a variation of the resistance of the support wires.

The constant current mode of the anemometer unit is employed to find sensor resistance as a function of temperature. The resistance of the sensor at the controlled bath temperature is measured by passing a low current through the anemometer bridge and balancing the bridge with a variable decade resistance. The bath temperature was measured with a thermometer whose accuracy of ±0.1 K was checked against thermometers calibrated at the National Bureau of Standards.

4. INSTRUMENTATION AND OPERATION

The cloud chamber used in this work has been described elsewhere [8]. Fig. 3 shows a schematic of the cloud chamber, and Fig. 4 is a schematic diagram of the data acquisition system. The hot wire unit included a Thermo-Systems, Inc., Model 1051-2 power supply, two Model 1053B utility anemometers, and two Model 1056 variable decade control resistances. Since these anemometers employ a 5:1 bridge ratio, 300 Ω precision resistors were added in series to each decade module. This modification allowed work with long hot wires which typically had resistances in excess of 79 Ω. Each output lead from the anemometers passed through a battery powered offset circuit before passing to a high gain amplifier. In this way zero suppression was achieved without surpassing the linearity limits of the galvanometers in the recording oscillograph (Consolidated Electrodynamics Corp. Model 5-124A).

Anemometer output voltages were calibrated against a Hewlett–Packard 34701A digital DC voltmeter and a mating 34740A display with a rated accuracy of ± (0.06% of reading + 0.02% of range). Pressure was measured by a diaphragm type sensor (CEC Type 4-313) whose movement is sensed by an unbonded, temperature-compensated strain gauge. The time response is faster than 5 ms. The pressure transducer was calibrated against a Wallace–Tiernan FA-135-173 mercurial barometer with a rated accuracy of 0.033% of full scale range. Ultra high purity argon was used

as the test gas. Initial temperature of the chamber was measured by establishing the resistance of the two hot wires prior to setting the overheat. A calibrated thermocouple in the test section was used to verify these readings. Piston velocities typically were of the order of 6 m/s, and the pressure decreased 40 kPa from an initial value near 100 kPa in less than 0.2 s.

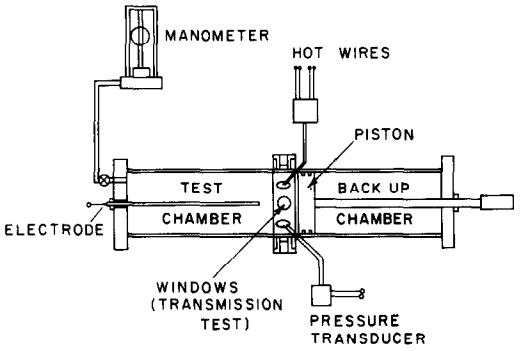

FIG. 3. Schematic diagram of expansion chamber.

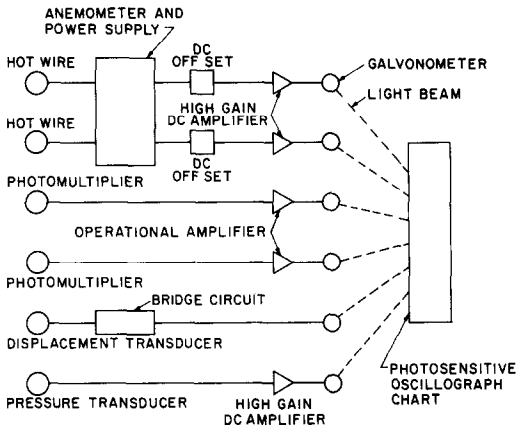

FIG. 4. Data acquisition system.

The most sensitive measurements were those of anemometer voltage, and CEC Model 7-317 galvanometers were installed for adequate time response. A square wave generator was used to optimize the anemometer time response through adjustment of the amplifier reference voltage. Bridge. stability was achieved through a matching of coaxial cables between the anemometer and control resistance against the supply cables from the anemometers to the hot wires. Further improvements here would be possible by the installation of variable inductors between the control decades and the anemometers. Proper inductive matching is more critical than capacitative optimization of the bridge [9]. The time response characteristics are diagnosed by subjecting the anemometer control resistance to a square wave signal and observing the anemometer output on an oscilloscope. These tests showed that the time response of the anemometers with the final cable configuration necessary for stable operation was about 0.2 ms.

5. ERROR ANALYSIS

The limitations of this dual wire technique are made evident by an error analysis of equation (6). We assume for simplicity that experimental errors in wire voltages, temperature settings, and temperature dependence of the convective heat-transfer coefficient are uncorrelated. In the analysis, the parameter ΔT_∞ is written as a function of parameters $x_1, x_2, \ldots, x_n$,

$$\Delta T_\infty = T_0 - T_\infty = y(x_1, x_2, \ldots, x_n). \tag{27}$$

The uncertainty of ΔT_∞ is then a geometric sum of the uncertainties of the uncorrelated parameters of form

$$\varepsilon^2_{\Delta T_\infty} = \sum_{i=1}^{n} I_i^2 \varepsilon_i^2 \tag{28}$$

where $\varepsilon_i = \Delta x_i / x_i$ and $I_i = x_i(\partial y/\partial x_i)/y$. Thus ε_i is the relative error of a given parameter x_i, and I_i is the corresponding influence coefficient. Applying this procedure to the basic relation equation (6) yields the following

$$\varepsilon^2_{\Delta T_\infty} = I_A^2 \varepsilon_A^2 + I_B^2 \varepsilon_B^2 + I_P^2 \varepsilon_P^2 \tag{29}$$

where ε_A, ε_B and ε_P are the relative errors of the quantities ΔT_A, ΔT_B and $\mathscr{P}_r$ and the influence coefficients are given by

$$I_A = -\frac{1}{\dfrac{1}{\mathscr{P}_r}\dfrac{\Delta T_B}{\Delta T_A} - 1}, \tag{30}$$

$$I_B = +\frac{1}{1 - \dfrac{\mathscr{P}_r \Delta T_A}{\Delta T_B}} \tag{31}$$

and

$$I_P = -\frac{1}{\mathscr{P}_r - 1}\frac{\dfrac{\Delta T_B}{\Delta T_A} - 1}{\dfrac{\Delta T_B}{\mathscr{P}_r \Delta T_A} - 1}. \tag{32}$$

In our recent testing we have found the values $\Delta T_A \approx 10$ K and $\Delta T_B \approx 35$ K to be advantageous.

6. SAMPLE DATA

Figure 5 is a tracing of a test chart for the expansion of dry argon. The traces for the anemometer bridge output voltages and the pressure transducer are noted. The smooth behavior of the anemometer voltages is notable as an indicator of laminar flow in the interior of the chamber during this early period of the expansion. Table 1 shows the temperature found from the hot wire method as $(T_0 - T_\infty)_{\text{obs}}$ compared with the value of this quantity derived independently from the observations of pressure and the use of the isentropic relationship to give

$$(T_0 - T_\infty)_{\text{is}} = T_0[1 - (p/p_0)^{\gamma - 1/\delta}]. \tag{33}$$

The pressures p are the measured values, γ is taken as 1.667 for argon and the subscript 0 refers to the conditions at the beginning of the run. The predicted uncertainty $\varepsilon_{\Delta T_\infty}$ is larger than the observed value.

Table 1. Data for expansion of dry argon

t(ms)	p(kPa)	$(T_0 - T_\infty)_{is}$ (K)	$(T_0 - T_\infty)_{obs}$ (K)	$(\varepsilon_{\Delta T_\infty})_{obs}$	$(\varepsilon_{\Delta T_\infty})_{pred}$
50	96.9	8.1	7.3	0.099	0.195
60	92.4	13.6	11.6	0.074	0.139
70	88.4	18.5	17.0	0.081	0.112
80	83.6	24.7	23.6	0.044	0.097

$T_0 = 297.5$ K; $T_A = 316.5$–316.0 K; $P_0 = 103.9$ kPa; $T_B = 332.8$–332.5 K.
Notes:
1. $(\varepsilon_{\Delta T_\infty})_{pred} \approx [\Sigma I_i^2 \varepsilon_i^2]^{1/2}$ with $\varepsilon_p = 0.01$ and uncertainties in ΔT_A and $\Delta T_B = 0.4$ K.
2. $(\varepsilon_{\Delta T_\infty})_{obs} = [(\Delta T_\infty)_{obs} - (\Delta T_\infty)_{is}]/(\Delta T_\infty)_{is}$.

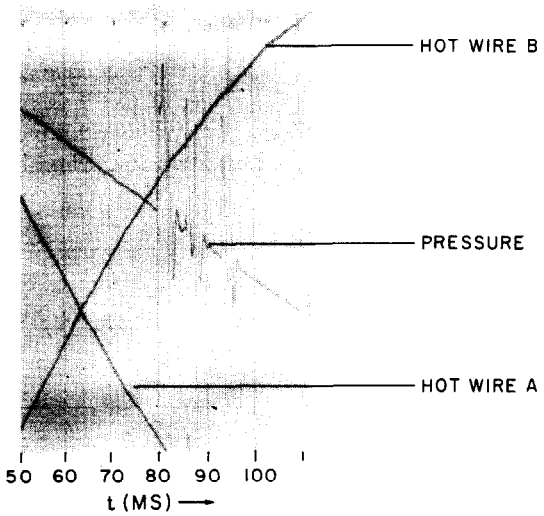

FIG. 5. Data trace for expansion of pure argon.

Table 2. Data for expansion of water-saturated argon (final droplet concentration is $0.11 \times 10^{+12}$ m^{-3})

t(ms)	T_∞(K)	p(kPa)
57.5	271.1	82.0
60.0	269.0	80.7
62.5	267.2	79.6
65.0	266.9	78.7
67.5	266.3	77.7
70.0	268.7	77.2
72.5	269.7	76.8

$T_0 = 298.3$ K; $P_0 = 104.7$ kPa;
$T_A = 316.8$ to 316.7 K; $T_B = 333.2$ K.

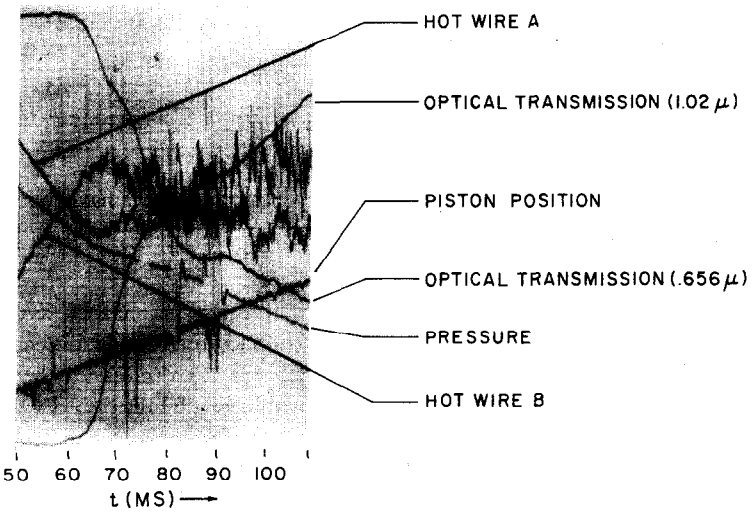

FIG. 6. Data trace for expansion of mixture of water vapor and argon.

Figure 6 is the test trace for argon initially saturated with water vapor. In addition to anemometer voltages and pressure, two optical signals and a piston displacement signal are displayed. The pressures and temperatures derived from Fig. 6 are presented in Table 2. A temperature minimum is reached at $t \sim 67.5$ ms, and the pressure trace changes slope between 65.0 and 67.5 ms. These effects are due to the evolution of latent heat by the growing droplets. The temperature extremum, pressure slope change, and optical transmission change are all associated with a finite duration nucleation pulse. The rapid oscillations of the signals from the sensors during and subsequent to the nucleation pulse probably caused by the impingment on the sensor of the droplets which are warmer than the vapor–gas mixture. These measurements have im-

portant implications on the diagnosis of the particle production and growth rates associated with nucleation.

7. CONCLUSION

The application of a dual hot wire temperature sensing technique to transient, supersaturated gas flows has been demonstrated. Cloud chamber temperatures for the first time can be measured during the nucleation process. The technique is useful in observation of temperature during the nucleation pulse itself, in studies of droplet growth subsequent to nucleation, and in quantitative observations of deviations from ideality of supersaturated gases in a manner previously impossible. The latter is important not only for further developments in virial equations of state but also as experimental input to the theory of clustering prior to nucleation.

Acknowledgements—The authors thank Mr. Thomas A. Raso for providing technical assistance. The counseling of Mr. William R. Patterson III on electronic instrumentation is acknowledged with special thanks. This research was sponsored by the National Science Foundation under Grant ENG 74-01648 A01.

REFERENCES

1. R. A. Dobbins and T. I. Eklund, Application of the method of Laplace to the measurement of homogeneous nucleation rates, *Aerosol Sci.* **5**, 497–505 (1974).
2. E. F. Allard and J. L. Kassner, Jr., New cloud-chamber method for the determination of homogeneous nucleation rates, *J. Chem. Phys.* **42**, 1401–1405 (1965).
3. L. B. Allen and J. L. Kassner, Jr., The nucleation of water vapor in the absence of particulate matter and ions, *J. Colloid Interface Sci.* **30**, 81–93 (1969).
4. D. C. Collis and M. J. Williams, Two-dimensional convection from heated wires of low Reynolds numbers, *J. Fluid Mech.* **6**, 357–384 (1959).
5. J. O. Hinze, *Turbulence*, Chapter 2. McGraw-Hill, New York (1959).
6. H. Lowell, Design and applications of hot-wire anemometer for steady-state measurements at transonic and supersonic speeds, NACA TN 2117 (1950).
7. C. D. Hodgman, *Handbook of Chemistry and Physics*, Chemical Rubber, Cleveland (1952).
8. J. E. Cole, III, R. A. Dobbins and H. Semerjian, Time-resolved measurement of droplet size and concentration in cloud chambers, *J. Appl. Meteor.* **9**, 684–689 (1970).
9. A. E. Perry and G. L. Morrison, A study of the constant temperature hot-wire anemometer, *J. Fluid Mech.* **47**, 577–599 (1971).

APPENDIX A

Resistance Correction Due to Input Bias Voltage

In Part 2 it was noted that the function of the amplifier is to maintain a nearly zero voltage difference between points A and C of the bridge circuit shown in Fig. 1. However, the feedback circuit employs a small voltage difference ($V_{ref}/\mathscr{A}$) between points A and C against which the bridge imbalance is to be sensed and corrected. Therefore, the bridge in the run mode is actually always unbalanced by a small voltage which causes a slight deviation of wire resistance from the perfectly balanced condition. This deviation is designated as ΔR^{cor}. Since the arms of the bridge circuit serve as two voltage dividers (see Fig. 1) it follows that the output voltage V is given by

$$V = \mathscr{A}\left(\frac{R_4}{R_1+R_4} - \frac{R_3}{R+R_c+R_3}\right)V + V_{ref} \qquad (A.1)$$

where

$$R = R_0 + \Delta R^{ap} + \Delta R^{cor}$$
$$R_1 = 5(R_0 + \Delta R^{ap} + R_c).$$

Thus R_0 is the cold resistance of the sensor as measured in the "standby" mode, $R_0+\Delta R^{ap}$ is the nominal hot resistance of the sensor in the "run" mode and $R = R_0 + \Delta R^{ap} + \Delta R^{cor}$ is the actual resistance of the sensor in the "run" mode.

Inserting the above values of R and R_1 into equation (A.1) and simplifying the result by noting that $\Delta R^{cor} \ll R_0 + \Delta R^{ap} + R_c$, we find the correction to the sensor resistance owing to bridge imbalance as

$$\Delta R^{ccr} = \left(\frac{V_{ref}}{V} - 1\right)\frac{(R_0 + \Delta R^{ap} + R_c + R_3)^2}{\mathscr{A}R_3}. \qquad (A.2)$$

Thus $\Delta R^{cor} \to 0$ as $\mathscr{A} \to \infty$.

The amplification $\mathscr{A}$ can be determined by a series of tests in which the output voltage is observed while the sensor overheat is increased. From equations (1) and (3) we find, for each anemometer unit,

$$\frac{V}{\left[\dfrac{R-R_0}{R_0}\dfrac{(R+R_c+R_3)^2}{R}\right]^{1/2}} = \left(\frac{hS}{\alpha}\right)^{1/2} \qquad (A.3)$$

where the sensor resistance R includes the proper correction owing to the bridge imbalance ΔR^{cor} calculated from equation (A.2). Since hS/α is constant for low overheats, the left side of equation (A.3) will be constant for various values of ΔR^{ap} if R is calculated with the proper amplification. A rapidly-converging trial and error procedure was used to calculate $\mathscr{A}$ assuming its initial value to be 10^{+4}. The tests to evaluate $\mathscr{A}$ were conducted at low power levels wherein the sensor was cooled only by natural convection and at higher power levels in a small calibration wind tunnel which duplicated the velocity range achieved in the test chamber. In both cases the same values of amplification, 8800 and 10 200 with $V_{ref} = 9.0$ V, were obtained for the two anemometer units that we employed. If a high overheat is used in the tests to determine amplification then the right side of equation (A.3) will vary because of the indirect dependence of h on film temperature. Potentially this dependence can be investigated by systematic tests at high values of overheat.

Once the amplification has been measured, the value of ΔR^{cor} can be calculated from equation (A.2) for a prescribed cold resistance R_0, overheat resistance ΔR^{ap}, reference voltage V_{ref}, and bridge output voltage V.

APPLICATION DE L'ANEMOMETRE A FIL CHAUD A LA MESURE DE TEMPERATURE DANS LES ECOULEMENTS GAZEUX INSTATIONNAIRES

Résumé—On décrit et utilise l'application de l'anémomètre à fil chaud pour la mesure de la température dans les écoulements gazeux instationnaires. Dans cette analyse, on inclut et on discute les corrections dues aux propriétés du gaz qui dépendent de la température et aussi aux pertes de chaleur par les supports du fil. On définit des critères pour minimiser les erreurs et on précise le calibrage statique des fils. On considère les caractéristiques opérationnelles de l'anémomètre et par une analyse des erreurs, on détermine leurs principales sources. On donne des résultats concernant les détentes de l'argon sec et de l'argon saturé d'eau dans une chambre de Wilson.

DIE ANWENDUNG DES HITZDRAHTANEMOMETERS ZUR TEMPERATURMESSUNG IN INSTATIONÄREN GASSTRÖMUNGEN

Zusammenfassung—Es wird die Anwendung des Hitzdrahtanemometers zur Temperaturmessung in instationären Gasströmungen beschrieben. Die Temperaturabhängigkeit der Stoffwerte des Gases und die Wärmeverluste an den Hitzdrahtenden werden mit berücksichtigt. Zur Minimisierung der Fehler und zur Ermöglichung einer statischen Kalibrierung der Drähte werden Auslegungskriterien angegeben. Es wird auf die Betriebscharakteristik des Anemometers eingegangen. Mit Hilfe einer Fehlerrechnung werden die wichtigsten Verbesserungsmöglichkeiten aufgezeigt. Für die Expansion von trockenem Argon und von mit Wasser gesättigtem Argon in einer Wilsonschen Nebelkammer werden Versuchsaufzeichnungen und reduzierte Daten angegeben.

ИЗМЕРЕНИЕ ТЕМПЕРАТУРЫ НЕСТАЦИОНАРНЫХ ПОТОКОВ ГАЗА С ПОМОЩЬЮ ПРОВОЛОЧНОГО ТЕРМОАНЕМОМЕТРА

Аннотация — Разработан и описан способ измерения температуры в неустановившихся потоках газа с помощью проволочного термоанемометра. Обсуждаются поправки, вводимые на зависящие от температуры физические свойства газа и утечки тепла через державки. Разработаны расчетные критерии, позволяющие минимизировать ошибки и проводить статическую калибровку проволочек анемометра. Рассматриваются рабочие характеристики термоанемометра. Проведенный анализ ошибок указывает пути совершенствования предложенного метода. Проведены измерения процесса расширения сухого и насыщенного водяным паром аргона в камере Вильсона.